SLOW HILLSLOPE PROCESSES ON EQUATORIAL MARS AS REVEALED BY THE TOPOGRAPHIC DIFFUSIVITY OF KM-SCALE CRATER RIMS. C. I. Fassett[1], W. A. Watters[2], and E.T. Chickles[2].[1]NASA Marshall Space Flight Center, [2]Dept of Astronomy, Wellesley College. (caleb.i.fassett@nasa.gov)

Introduction and Summary: Erosion rates on Mars have been estimated in many past studies [e.g., 1-5]. Erosion has been inferred to be quite slow by terrestrial standards, consistent with the basic observation that martian landforms often survive billions of years. However, there is significant complexity in martian terrain modification and geomorphic evolution. The erosion rates that have been determined are a function of measurement scale, temporal baseline, geologic setting, and the type of measurement. Thus, it merits additional assessment.

We have been pursuing this problem by looking at the changes in morphometry and morphology of craters exposed to modification on the martian surface [see also companion abstract, 6]. Last year, we used the survival of crater ejecta as a proxy for the geographic variability in erosion [7] (though this was not presented formally due to the pandemic and meeting cancellation). Here, we focus on the history of rim erosion with time. Specifically, we estimate the topographic diffusion of crater rims and use this as a metric for how modified they are [e.g., 8]. These diffusive states are then tied to model ages based on crater population statistics. Combined, this allows us to assess rim modification rates with time.

The rim degradation history we infer here shows that crater rims are modified surprisingly slowly in Mars's equatorial regions. The thin atmosphere of Mars is apparently sufficiently thick to limit the efficiency of rim modification by small impacts, which is important on airless bodies [e.g., 9]. Mars also lacks bioturbation [e.g., 10, 11] or rain splash [e.g. 12], which are forcing mechanisms for diffusive hillslope modification on Earth. The result is that crater rims – and probably other hillslopes (e.g., the Columbia hills, valley walls) – have been eroded more slowly on Mars than similar landforms on the Moon, at least in recent epochs. Most of the modification of topographic relief for craters is *not* from localized rim erosion, but from non-local, non-diffusive eolian infill, a comparatively fast process [1-5]. This crater infilling is dominated by external mobile sediment, which has implications for how regolith evolution differs on the Moon and Mars.

Method: We generated more than 80,000 CTX digital terrain models (DTMs) from the available stereo CTX data (as of March 2019) using the Ames Stereo Pipeline [13]. Image pairs were chosen based on criteria outlined by [14] from images with reasonably significant overlap. The quality of resulting DTMs varied widely, as expected given they were not necessarily targeted for stereo. This was carefully taken into account during analysis by establishing quality metrics and excluding low quality DTMs. In equatorial latitudes (30°S to 30°N), all the D=1–5 km craters in the Robbins catalog [15] that had coverage had stereo CTX DTMs were identified and radial profiles for the craters were extracted from the DTMs after removing background topography. Some craters were covered by more than one DTM, in which case the highest quality one was used. We used the manual classification discussed last year [7] to exclude exhumed craters, probable secondaries, and non-craters from further analysis.

On the lunar maria [8], diffusive model profiles commonly match the topography of craters from their center to outside their rim. This is almost never the case on Mars (except for some extraordinarily fresh craters, <1% of the population). Instead, as mentioned earlier, the floors of even modestly modified craters are ubiquitously infilled (non-locally, since the crater rims remain intact). For this reason, to characterize the evolution of the rim alone, we calculated the best-fit diffusive model (κt_{rim}) for each radial profile from $0.75R_{rim}$ to $1.25R_{rim}$ (e.g. Fig. 1).

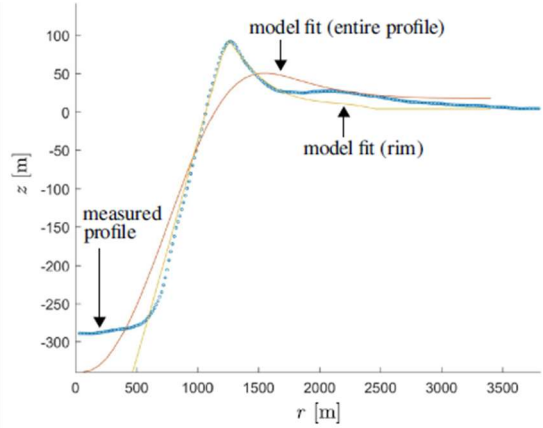

Figure 1. Robbins [15] crater 10-002207 (D~2.5 km). The model rim diffusive profile (yellow) fits the rim well (R^2=0.99), but it is impossible to fit the entire profile with a closely matching model (orange) because of non-diffusive infill.

After fitting model rim diffusive profiles for all the high-quality data and subsetting the data as described above, we excluded craters whose κt_{rim} fits were R^2<0.9. The resulting dataset had 14,195 craters distributed across the martian equatorial region. The next step was

to tie these estimated rim diffusion states to their exposure time. We used the same basic methods as in [8]. For each crater with an inferred κt_{rim}, the local crater density N(1) was extracted from [15] based on a moving neighborhood of 100 km radius. Craters were then sorted by local N(1), and binned by this parameter into n = 100 crater bins. For each bin, 10th-, 25th-, 50th-, 75th-, and 90th-percentiles of the degradation state distribution were then determined. The median κt_{rim} (50th-percentile crater degradation state at a given crater density) and the interquartile range of crater degradation states increase as crater density (age) increases, as expected.

The measured frequencies were then translated into a Neukum/Ivanov model age [16], making the approximation that the crater with the 10th-percentile degradation state for its surface formed at an age equivalent to 10% of the region's frequency; in other words, after 90% of the other craters in that area's population had already been accumulated (and likewise for the 25th percentile, 50th percentile, etc.). This assumption is logical if crater degradation monotonically increases from least degraded to most degraded, but is unlikely to hold strictly.

Results: A representation of the typical sequence of rim degradation on Mars with time is shown in Figure 2a. The data was fit with a line for the period t <3.05 Ga (R^2 = 0.75) and with an exponential for t> 3.05 (R2 = 0.58). The 90th-percentile points are not included in this calibration as they systematically fall above this best-fit curve; the same thing happened on the Moon [8]. Because Fig. 2a shows κt_{rim} as a function of t, its slope at any point is the rim diffusivity κ.

These results imply that over most of the Amazonian (<3 Ga), the rim diffusivity on Mars averaged a factor of ~6× lower than the diffusivity of the Moon. In earlier periods, when the crater flux was higher, the rim diffusivity on Mars increased, as it did also on the Moon. These data imply a radical change occurred in rim modification behavior on Mars happened ~3-3.4 Ga, in the earliest Amazonian or at the Hesperian/Amazonian boundary. This apparent upturn in rim diffusivity at >3 Ga is unlikely to be an artifact, though the coincident timing between the Moon and Mars may be a consequence of the Mars' crater chronology being derived from the Moon's.

Acknowledgments: This work was supported in part by NASA MDAP award NNX15AM40G. We are grateful to Hallie Pimperl, Laura Chin, and Abby Surlet for their contributions.

References: [1] Hartmann, W.K. (1971), *Icarus*, *15*, 410–428. [2] Golombek, M.P., Bridges, N.T., (2000), *JGR-Planets, 105*, 10.1029/1999JE001043. [3] Golombek, M.P. et al. (2006), *JGR-Planets*, *111*, 10.1029/2006JE002754. [4] Golombek, M.P. et al. (2014), *JGR-Planets*, *119*, 10.1002/2014JE004658. [5] Sweeney, J. et al. (2018), *JGR-Planets*, *123*, 10.1029/2018JE005618. [6] Watters, W.A. et al. (2021), this meeting. [7] Fassett, C.I. et al. (2020), *LPSC 51, 1586;* eposter. [8] Fassett, C.I., Thomson, B.J. (2014), *JGR*, *119*, 10.1002/2014JE004698. [9] Minton, D.A. et al. (2019), *Icarus*, *326*, 63-87. [10] Gabet, EJ. (2000). *ESPL*, *25*, 1419–1428. [11] Roering, J.J. et al. (2002). *Geology*, *30*, 1115-1118. [12] Sweeney, K. E. et al. (2015), *Science, 349*, 51–53. [13] Beyer, R.A. et al. (2018), *Earth and Space Science*, *5*, 10.1029/2018EA000409. [14] Becker, K.J. et al. (2015), *LPSC*, *46*, 2703. [15] Robbins, S.J. & Hynek, B. (2012), *JGR-Planets*, *117*, 10.1029/2011JE003966. [16] Ivanov, B. A. (2001), *Space Sci. Rev., 96,* 87–104. [17] Fassett et al. (2018), LPSC 49, 1502.

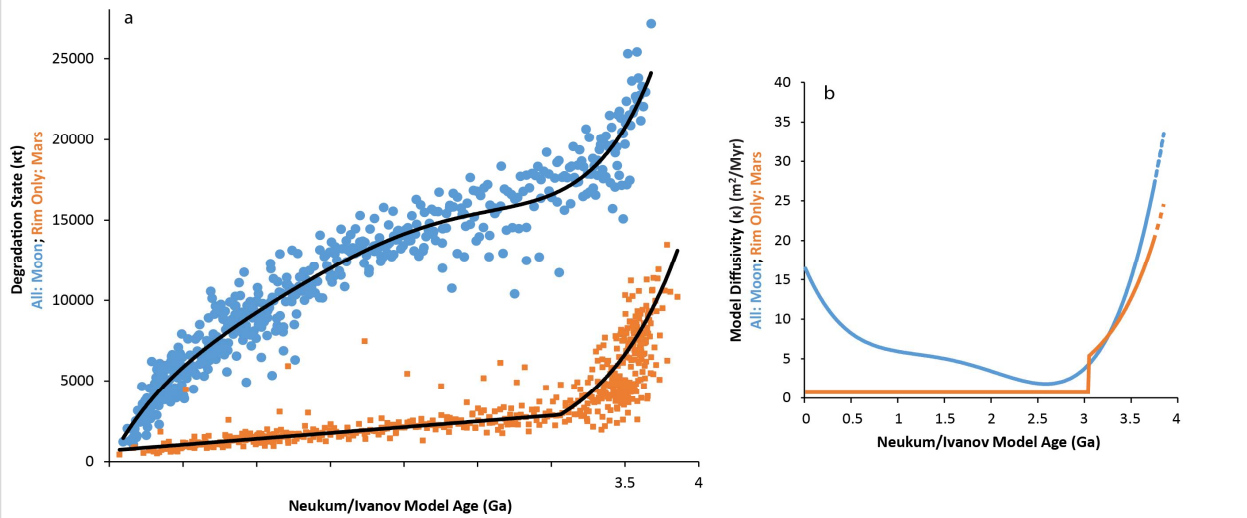

Figure 2. (a) Diffusive states of craters with time (based on a crater statistics-based calibration), and (b) inferred diffusivity (the derivative of the models fit in (a)). The model fits to crater profiles on the Moon (blue) [8, 17] are for the whole crater profile, and Mars (orange) are strictly for the crater rim. This sequence implies craters on Mars from the early Amazonian (~3 Ga) often have appreciable rims, while craters of similar age on the lunar maria have mostly lost their entire rims.